

# Characterization of the Residues Involved in the Human $\alpha$ -Thrombin–Haemadin Complex: An Exosite II-Binding Inhibitor

John L. Richardson,<sup>\*,‡</sup> Pablo Fuentes-Prior,<sup>‡</sup> J. Evan Sadler,<sup>§</sup> Robert Huber,<sup>‡</sup> and Wolfram Bode<sup>‡</sup>

Max-Planck-Institut für Biochemie, D-82152 Martinsried, Germany, and Howard Hughes Medical Institute, Washington University School of Medicine, St. Louis, Missouri 63110

Received August 3, 2001; Revised Manuscript Received October 9, 2001

**ABSTRACT:** Haemadin is a 57-amino acid thrombin inhibitor from the land-living leech *Haemadipsa sylvestris*, whose structure has recently been determined in complex with human  $\alpha$ -thrombin. Here we communicate the effect of ionic strength on the kinetics of the inhibition of human  $\alpha$ -thrombin by haemadin, by using thrombin mutants modified in exosite II. Data analysis has allowed both the ionic and nonionic binding contributions to be ascertained, with the nonionic component being virtually the same for all of the thrombins that have been examined, while the ionic binding energy contributions varied from molecule to molecule. In the case of the native human  $\alpha$ -thrombin–haemadin complex, ionic interactions contribute  $-17$  kJ/mol to the Gibbs free energy of binding, this being the equivalent of up to six salt bridges. These salt bridges make up 20% of the total binding energy at zero ionic strength, and this has been attributed to the C-terminal tail alone. In addition, the contributions of the N-terminal and C-terminal regions of haemadin to its tight binding have been ascertained by using derivatives of both haemadin and thrombin. Limited proteolysis using formic acid produced haemadin cleaved between residues 40 and 41, removing the majority of the C-terminal tail. This truncated haemadin displayed a 20000-fold reduced affinity for thrombin, and was no longer a tight binding inhibitor. A form of thrombin in which the active site serine has been blocked by diisopropyl fluorophosphate binds to haemadin, but with a 72000-fold reduced affinity, indicating that the N-terminus is more important than the C-terminus for strong binding.

Thrombin is a trypsin-like serine protease, which has a central role in the processes of both thrombosis and hemostasis. In the process leading to clot formation,  $\alpha$ -thrombin performs several major roles. First, it converts soluble fibrinogen into fibrin, and second, it activates the transglutaminase factor XIII, which subsequently cross-links adjacent fibrin monomers (1). Additionally, via proteolytic activation of G protein-coupled PARs<sup>1</sup> and of the unique platelet receptor GPIb-IX-V, thrombin induces platelet aggregation (2–4). Thrombin also promotes its own production by activating essential nonenzymatic cofactors V and VIII (5) as well as factor XI (6). Conversely, thrombin, when bound to the endothelial membrane receptor thrombomodulin, becomes a potent activator of both protein C (7) and the procarboxypeptidase thrombin-activatable fibrinolysis inhibitor (8), which leads to the simultaneous deactivation of the coagulation cascade and the inhibition of fibrinolysis. Specific features of thrombin's structure include not only a

rather inaccessible active site due to two striking loop insertions but also two patches of positive surface potential which play a critical role in its binding to substrates and inhibitors: the fibrinogen-recognition exosite (also termed anion-binding exosite I) and the heparin-binding exosite (or anion-binding exosite II) (9).

Haemadin is a 57-amino acid peptide first identified in the saliva of the land-living leech *Haemadipsa sylvestris* (10), which binds tightly to thrombin with a  $K_i$  of  $2.44 \times 10^{-13}$  M. In the X-ray crystal structure of the human  $\alpha$ -thrombin–haemadin complex, which we have recently determined (11), haemadin binds to the active site of thrombin, with its N-terminus forming a parallel  $\beta$ -sheet with thrombin residues Ser214–Gly216.<sup>2</sup> Additionally, haemadin makes many other contacts with the active site, including a salt bridge between arginine 21 (the suffix “I” identifies haemadin residues) and aspartate 189 of thrombin in the S1 pocket.<sup>3</sup> The compact core of haemadin (residues 10–37) makes further interactions mainly through its A and C loops with the 60- and 96-loops of thrombin, while the acidic C-terminal tail covers the heparin binding site of thrombin (exosite II). Due to additional contacts in the crystal structure of the C-terminal tail with exosite I of a neighboring thrombin molecule, the exact nature of the binding of the C-terminal tail of haemadin to exosite II was not fully ascertained, and this study seeks to address this question.

\* To whom correspondence should be addressed. E-mail: richards@biochem.mpg.de.

<sup>‡</sup> Max-Planck-Institut für Biochemie.

<sup>§</sup> Washington University School of Medicine.

<sup>1</sup> Abbreviations: DIPF, diisopropyl fluorophosphate; DIP-thrombin, diisopropylphosphorylthrombin; HPLC, high-performance liquid chromatography; HM2(1–41), residues 1–41 of hirudin variant 2 from *Hirudinaria manillensis*; haemadin(1–40), haemadin residues 1–40; hirudin(1–43), residues 1–43 of hirudin from *H. medicinalis*; MES, morpholineethanesulfonate; PARs, protease-activated receptors; PEG, poly(ethylene glycol); S-2238, D-Phe-pipecolyl-Arg-p-nitroanilide; TFA, trifluoroacetic acid; Tos-GPR-AMC, tosyl-Gly-Pro-Arg-aminomethyl coumarin; Tris, tris(hydroxymethyl)aminomethane.

<sup>2</sup> The numbering of thrombin is based on chymotrypsinogen numbering (9).

<sup>3</sup> S1 designates the corresponding subsite for the P1 residue of a substrate; for a detailed explanation, see ref 12.

The effect of ionic strength on the kinetics of inhibition of human  $\alpha$ -thrombin, and a number of mutant thrombins, with haemadin has been examined using a modification of the Debye–Hückel theory which has been shown to be applicable at higher ionic strengths (13). This treatment has allowed the binding energy of haemadin for each of the complexes that has been examined to be calculated and to be divided into ionic and nonionic contributions. In addition, the  $k_{on}$  at infinite ionic strength has been ascertained, as well as the average distances between the charged groups in the complex of haemadin with native thrombin, and with four other thrombin mutants. Additionally, limited proteolysis of haemadin and the use of a chemically altered thrombin have been used to probe aspects of the structure and evaluate the importance with respect to tight binding of both the N- and C-terminal regions of haemadin, at both low and high ionic strengths.

## EXPERIMENTAL PROCEDURES

**Materials.** Human  $\alpha$ -thrombin was prepared from frozen plasma as previously described (14) and was pure as judged by gel electrophoresis and sequencing. Thrombin mutants where basic residues have been mutated to glutamic acid were prepared as previously described (15, 16). Thrombins used were not less than 95% active as determined by active site titration (17) using 4-methylumbelliferyl *p*-guanidobenzoate. Haemadin was prepared according to the method of Strube et al. (10). All other reagents were of the highest purity available commercially.

**Amidolytic Assays of Thrombin.** Slow and tight binding assays were performed at 25 °C as previously described (10). Tight binding assays were performed with a final concentration of 500 pM human  $\alpha$ -thrombin (or mutant), being preincubated for more than 30 min with inhibitor (0.4–2.4- $[E_0]$ ), in 50 mM Tris-HCl (pH 8.3), 50 mM NaCl, and 0.1% PEG6000. A plot of velocity against concentration of haemadin (seven points) was fitted using nonlinear regression to eq 1 to obtain the  $K_i$ . This procedure was repeated using varying substrate concentrations (100–500  $\mu$ M S-2238), and the resulting  $K_i$  values (five points) were plotted against substrate concentration using weighted linear regression to eq 2, with the points weighted to the inverse square of their standard errors to obtain the  $K_i$ .

Slow binding assays were conducted using 25  $\mu$ M Tos-GPR-AMC as a substrate in 50 mM Tris-HCl (pH 8.3), 50 mM NaCl, and 0.1% PEG6000 with varying inhibitor concentrations (15–30 $[E_0]$ ). The reaction was started by the addition of 10 pM human  $\alpha$ -thrombin or mutant thrombin (final concentration), and a plot of the amount of product formed against time (33 points) was fitted using nonlinear regression to eq 3 to obtain the  $k_{app}$ . A plot of  $k_{app}$  against inhibitor concentration (four points) was fitted to eq 4 to obtain the  $k_{on}$ . The  $k_{off}$  was calculated from the  $K_i$  value and the  $k_{on}$  value by using the equation  $K_i = k_{off}/k_{on}$ .

Ionic strength was calculated assuming a  $pK_a$  of 8.1 for Tris at 25 °C (18), with the ionic strength being checked by measuring the conductance of the solutions. In all cases, the ionic strength measured was within 5% of the theoretical value.

The kinetic constants for each of the mutant thrombins toward substrates S-2238 and Tos-GPR-AMC were deter-

mined using a concentration of thrombin of  $5 \times 10^{-10}$  M, with the concentrations of both substrates (S-2238 and Tos-GPR-AMC) being varied from 5 to 25  $\mu$ M. The initial velocities that were obtained (five points) were fitted to the Michaelis–Menten equation using linear regression (19).

**Haemadin Cleavage and Kinetics.** Haemadin was cleaved between residues Asp40I and Pro41I using the formic acid method to produce a truncated form, haemadin(1–40), which has been isolated to homogeneity as described below. A solution of haemadin (175  $\mu$ g/mL) had formic acid added until it was a 70% (v/v) formic acid solution and was heated at 40 °C for 48 h. The resultant solution was diluted with 20 volumes of water and applied to a reverse phase source 5RPC ST column (Amersham Pharmacia Biotech), where it was eluted using a linear gradient from 10 to 90% acetonitrile/water with 0.1% TFA on an HPLC system. The resultant protein was judged pure from protein sequencing data and from mass spectral analysis ( $m/z$  4198.7,  $M_{calc} = 4200.1$ ). The concentration of the inhibitor as determined for usage in the experiments described below was determined by UV absorption using a UVIKON 943 double-beam spectrophotometer. The absorption coefficient for the inhibitor ( $\epsilon_{280} = 0.696 \text{ mg}^{-1} \text{ cm}^2$ ) was determined using molecular absorption coefficients of 1280 and 120  $\text{M}^{-1} \text{ cm}^{-1}$  for tyrosine and cysteine residues, respectively (20). In a similar way, the concentration of intact haemadin was determined for use in the experiments described using the same method, with the absorption coefficient ( $\epsilon_{280} = 0.468 \text{ mg}^{-1} \text{ cm}^2$ ) being calculated in the same manner.

$K_i$  values for the human  $\alpha$ -thrombin–haemadin(1–40) complex were determined as follows. Solutions of  $5 \times 10^{-10}$  M thrombin in 50 mM Tris-HCl (pH 8.3), 50 or 500 mM NaCl, and 0.1% PEG6000 at 25 °C with varying concentrations of haemadin(1–40) were taken, and the assays were started by the addition of substrate. Initial rate velocities were recorded at four different substrate concentrations (from 20 to  $125 \times 10^{-6}$  M) and used to construct Dixon plots. The relationship of the inverse of the initial velocities versus inhibitor concentration [ $1-4 \times 10^{-8}$  M (four points)] was analyzed using linear regression, with the  $K_i$  values being determined by standard procedures using the equation which describes competitive inhibition (19). Associative rate constant ( $k_{on}$ ) values for the thrombin–haemadin(1–40) complex were determined using pseudo-first-order kinetics. A 500  $\mu$ L volume of a solution of  $1 \times 10^{-8}$  M haemadin(1–40) in 50 or 500 mM Tris-HCl (pH 8.3), 50 mM NaCl, and 0.1% PEG6000 was taken, and the assay was started by adding thrombin to a final concentration of  $1 \times 10^{-9}$  M. Every 5 min, a 25  $\mu$ L aliquot was taken and added to 225  $\mu$ L of 217  $\mu$ M S-2238 in the same buffer described above, where the initial velocity was measured. Alongside this reaction, a reaction without inhibitor was performed as a control. The initial velocity is proportional to the amount of uninhibited thrombin present in the assay, and obeys the equation  $V_i = V_0 \exp(-k_{app}t)$  (21). Nonlinear regression on velocities taken against time was fitted to this equation to give a value for  $k_{app}$ , and the  $k_{on}$  value was determined by dividing  $k_{app}$  by the inhibitor concentration.

**DIP-Thrombin Preparation and Kinetics.** DIP-thrombin was prepared by a modification of the method of Stone et al. (22). A solution of human  $\alpha$ -thrombin (12  $\mu$ M) in 55 mM NaCl and 0.5 mM MES (pH 6.0) was incubated at room

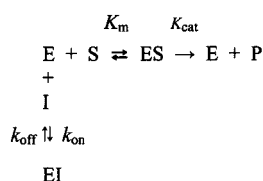
temperature with 1 mM diisopropyl fluorophosphate (DIPF) for 30 min. After this time, an aliquot was taken and tested for thrombin activity using the chromagenic substrate S-2238. If the thrombin activity was greater than 0.01% of the activity of the original solution, more DIPF was added until the concentration was 1 mM greater than it was previously, and after 30 min, the solution was reassayed for thrombin activity. This procedure was repeated until the thrombin activity was  $\leq 0.01\%$  of the original activity. The thrombin solution was then exhaustively dialyzed against 50 mM Tris-HCl (pH 8.3), 50 mM NaCl, and 0.1% PEG6000, and its concentration was determined by measuring its absorption at 280 nm according to the method of Fenton et al. (23).

The inclusion of DIP-thrombin in assays of steady state rates against inhibitor concentration (conducted as described previously in Amidolytic Assays of Thrombin) caused an increase in the  $K_i'$  which was linear when plotted against the concentration of DIP-thrombin added. The variation of the value of the dissociation constant obeyed eq 2 as would be expected for a competitive ligand. The  $K_i'$  derived from the steady state experiments without DIP-thrombin, divided by the slope of this plot [from 0 to 50 nM DIP-thrombin (six points)], gave a value of the  $K_i$  for the DIP-thrombin–haemadin complex.

**Peptide Synthesis and Kinetics.** The synthesis of amino-terminal peptides H-IRFGMGKV-NH<sub>2</sub> and H-IRFGMGKVP-NH<sub>2</sub> based on the first eight and nine amino acids of haemadin, respectively, was achieved by the solid phase method (1 mmol scale) employing the classical protocols for the *N*- $\alpha$ -Fmoc strategy. After cleavage from the resin, the products were precipitated with a methyl *tert*-butyl ether/hexane mixture, and the crude peptides were purified by preparative RP-HPLC eluted using a linear gradient from 0 to 100% of a 0.1% aqueous TFA/0.08% TFA mixture in CH<sub>3</sub>CN, with the products being obtained upon lyophilization. The resultant proteins were judged to be pure from mass spectral analysis ( $m/z$  905.6,  $M_{\text{calc}} = 905.5$ ) and ( $m/z$  1002.6,  $M_{\text{calc}} = 1002.6$ ).

$K_i$  values for human  $\alpha$ -thrombin–peptide complexes were determined as follows. Solutions of  $6.1 \times 10^{-9}$  M thrombin in 50 mM Tris-HCl (pH 8.3), 100 mM NaCl, and 0.1% PEG6000 at 25 °C with varying concentrations of each peptide were taken, and the assays were started by the addition of substrate. Initial rate velocities were recorded at a substrate concentration of  $150 \times 10^{-6}$  M and used to construct Dixon plots. The relationship of the inverse of the initial velocities versus inhibitor concentration [ $0$ – $500 \times 10^{-6}$  M (seven points)] was analyzed using linear regression, with the  $K_i$  values being determined by standard procedures using the equation which describes competitive inhibition (19).

**Theory and Data Analysis.** The inhibition of an enzyme in the presence of substrate can be illustrated by the following scheme where E is thrombin, S is substrate (S-2238 or Tos-GPR-AMC), I is haemadin, and P is products:



The dissociation constant of the inhibitor ( $K_i$ ) is given by  $k_{off}/k_{on}$ .

In the case of tight binding inhibition, where binding of the inhibitor causes a significant depletion in the amount of free inhibitor, the variation of the steady state velocity ( $v_s$ ) with the total inhibitor concentration ( $I_t$ ) is given by the following equation:

$$v_s = (v_o/2E_t)\{[(K_i' + I_t - E_t)^2 + 4K_i'E_t]^{0.5} - (K_i' + I_t - E_t)\} \quad (1)$$

where  $v_o$  is the velocity in the absence of inhibitor,  $E_t$  is the total enzyme concentration, and  $K_i'$  is the apparent inhibition constant (24).

In the case of competitive inhibition, the dissociation constant ( $K_i$ ) of a tight binding inhibitor can be calculated from the apparent inhibition constant ( $K_i'$ ) via the following equation:

$$K_i' = K_i(1 + S/K_m) \quad (2)$$

where  $S$  is the competing substrate concentration and  $K_m$  is the Michaelis constant of the substrate for the enzyme (24).

In the case of slow binding inhibition, the amount of product formed ( $P$ ) in a certain time ( $t$ ) is described by the following equation:

$$P = v_s t + (v_o - v_s)[1 - \exp(-k_{app}t)]/k_{app} + d \quad (3)$$

where  $v_s$  is the steady state velocity,  $v_o$  is the initial velocity,  $k_{app}$  is the apparent rate constant (unrelated to  $K_i'$ ), and  $d$  is a time displacement term inserted to account for the fact that at time zero the amount of product may not have been known accurately.

From the  $k_{app}$ , the constants  $k_{on}$  and  $k_{off}$  can be calculated from the equation below (25):

$$k_{app} = [k_{on}/(1 + S/K_m)]I + k_{off} \quad (4)$$

The standard Gibbs free energy of formation of the complex ( $\Delta G_b^\circ$ ) (also termed the binding energy) is given by the following equation where  $R$  is the gas constant and  $T$  is the absolute temperature:

$$\Delta G_b^\circ = RT \ln K_i \quad (5)$$

The  $\Delta G_b^\circ$  can be divided into an ionic component ( $\Delta G_{ion}^\circ$ ) and a nonionic ( $\Delta G_{nio}^\circ$ ) component:

$$\Delta G_b^\circ = \Delta G_{ion}^\circ + \Delta G_{nio}^\circ \quad (6)$$

From the Debye–Hückel theory, the value of  $\Delta G_{ion}^\circ$  will be dependent on the ionic strength ( $I$ ) according to the equation

$$\Delta G_{ion}^\circ = \Delta G_{ion0}^\circ \exp(-C_1 \sqrt{I}) \quad (7)$$

where  $\Delta G_{ion0}^\circ$  is the ionic interaction energy at an ionic strength of zero and  $C_1$  is a constant that is related to those terms in the Debye–Hückel screening parameter that are independent of ionic strengths, and the distance between the two charges (26).

However, Debye–Hückel theory is only applicable at low ionic strengths, and several semiempirical terms must be



introduced to account for deviations. One such treatment has been shown to be applicable to higher ionic strengths in the case of proteins (27–29):

$$\Delta G^\circ_{\text{ion}} = \Delta G^\circ_{\text{ion0}} [\exp(-C_1 \sqrt{I}) / (1 + C_1 \sqrt{I})] \quad (8)$$

Substitution of eqs 7 and 8 into eq 6 gives the following expression for the dependence of binding energy on ionic strength:

$$\Delta G^\circ_b = \Delta G^\circ_{\text{nio}} + \Delta G^\circ_{\text{ion}} [\exp(-C_1 \sqrt{I}) / (1 + C_1 \sqrt{I})] \quad (9)$$

In the case of ionic interactions, the  $k_{\text{on}}$  will also be dependent on ionic strength, and the following equation can be derived from eqs 7 and 8 to describe this dependence:

$$\ln k_{\text{on}} = (\ln k_{\text{on8}}) (-\Delta G^\circ_{\text{ion0}} / RT) [\exp(-C_1 \sqrt{I}) / (1 + C_1 \sqrt{I})] \quad (10)$$

where  $k_{\text{on8}}$  is the association rate constant at infinite ionic strength.

A simple way to evaluate ionic forces is to treat the solvent as being a continuum having a dielectric constant  $\epsilon$  (30):

$$\Delta G^\circ_{\text{ion}} = (L z_A z_B e^2) / (4\pi \epsilon_0 \epsilon d_{AB}) \quad (11)$$

where  $L$  is the Avogadro constant,  $z_A$  and  $z_B$  are the charges of the ions,  $e$  is the elementary charge,  $\epsilon_0$  is the vacuum permittivity,  $\epsilon$  is the effective dielectric constant of the solvent, and  $d_{AB}$  is the distance between the charge centers.

## RESULTS

Consideration of ionic strength effects for the Debye–Hückel theory requires that low ionic strengths be used. However, a modification of the Debye–Hückel theory, which has previously been shown to be applicable at higher ionic strengths (27–29) and has been applied in the case of thrombin (13), has proved to fit the data more accurately than the Debye–Hückel theory. The dissociative and associative rate constants for thrombin and four thrombin mutants were determined over a range of ionic strengths from 0.0695 to 0.5195; these higher ionic strengths were used to circumvent losses of protein which frequently occur at lower ionic strengths.

The kinetic constants of haemadin with human  $\alpha$ -thrombin, and with 10 other thrombin mutants, where a basic residue has been mutated to a glutamic acid, at an ionic strength of 0.0695 are shown in Table 1. The investigation of ionic interactions between the C-terminal tail of haemadin required that mutants of the heparin binding site (exosite II) be considered which, as shown in Table 1, have a significant effect on the  $K_i$  compared to that of native thrombin or other thrombin mutants. In addition to the mutants that have already been tested (11), the  $K_i$  values of another four mutants (K60fE, R75E, R169E, and K235E) were measured and their similarity in binding energy to native thrombin effectively ruled them out as being involved in thrombin–haemadin interactions. In addition, the  $k_{\text{on}}$  of human  $\alpha$ -thrombin, along with 10 mutants with haemadin, was measured at an ionic strength of 0.0695, and this enabled the  $k_{\text{off}}$  for all the thrombins to be determined. Both these figures are shown in Table 1 along with their standard deviations.

Table 1: Kinetic Constants of Thrombin Mutants at 0.05 M Tris (pH 8.3), 0.05 M NaCl, and 0.1% PEG6000 at 25 °C

	$K_i$ ( $\times 10^{-13}$ M)	fold increase relative to native	$k_{\text{on}}$ ( $\times 10^7$ M $^{-1}$ s $^{-1}$ )	$k_{\text{off}}$ ( $\times 10^{-5}$ s $^{-1}$ )
native	2.44 $\pm$ 0.14 <sup>a</sup>	1.00	9.32 $\pm$ 1.65	2.27 $\pm$ 0.42
K60fE	2.48 $\pm$ 0.57	1.02	10.5 $\pm$ 0.23	2.62 $\pm$ 0.60
R73E	3.37 $\pm$ 0.52 <sup>a</sup>	1.38	7.20 $\pm$ 0.39	2.42 $\pm$ 0.40
R75E	2.51 $\pm$ 0.73	1.03	9.46 $\pm$ 0.38	2.37 $\pm$ 0.70
R93E	24.1 $\pm$ 0.12 <sup>a</sup>	9.89	1.46 $\pm$ 0.38	3.51 $\pm$ 0.92
K149eE	2.34 $\pm$ 0.35 <sup>a</sup>	0.96	11.7 $\pm$ 0.57	2.73 $\pm$ 0.43
K169E	2.29 $\pm$ 0.63	0.94	9.78 $\pm$ 0.84	2.24 $\pm$ 0.65
R233E	7.33 $\pm$ 0.45 <sup>a</sup>	3.01	4.44 $\pm$ 0.49	3.25 $\pm$ 0.41
K235E	2.45 $\pm$ 0.41	1.01	9.15 $\pm$ 0.92	2.24 $\pm$ 0.43
K236E	4.22 $\pm$ 0.30 <sup>a</sup>	1.73	6.55 $\pm$ 0.30	2.77 $\pm$ 0.24
K240E	12.9 $\pm$ 0.87 <sup>a</sup>	5.30	2.70 $\pm$ 0.24	3.48 $\pm$ 0.39

<sup>a</sup> Denotes values previously determined in ref 11.

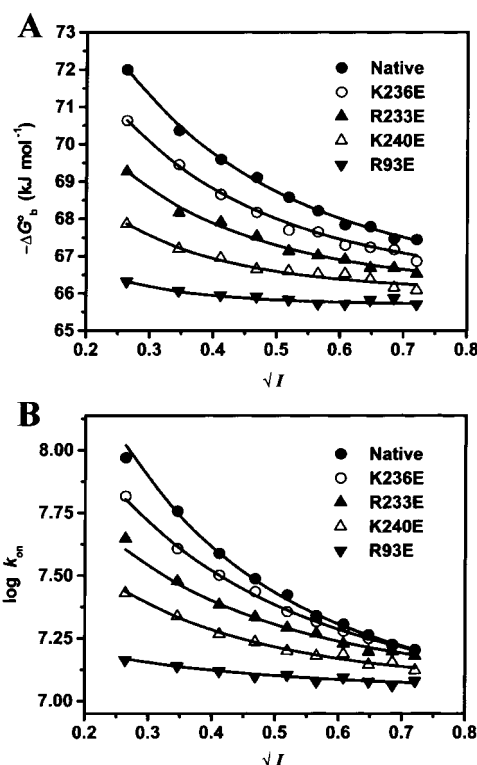


FIGURE 1: (A) Effect of ionic strength on the binding energies of complexes of haemadin with thrombin and thrombin mutants. The binding energies of thrombin or thrombin mutants in complex with haemadin are plotted against the square root of the ionic strength. Points are experimental ones derived from the  $K_i$  using eq 5, and the lines represent the best fit to eq 9 with the points weighted to the inverse square of their standard errors. (B) Effect of ionic strength on the associative rate constant  $k_{\text{on}}$  for association of haemadin with thrombin or thrombin mutants. Values of the associative rate constant are plotted against the square root of the ionic strength. Points are experimental, and the lines represent the best fit to eq 10 with the points weighted to the inverse square of their standard errors.

Of the exosite II mutants, which were implicated in haemadin binding as shown from their higher  $K_i$  values (compared to that of native thrombin) in Table 1 (R93E, R233E, K236E, and K240E), along with native thrombin, the effect of ionic strength on the  $K_i$  is shown in Figure 1A. As can be seen from the graph, the  $\Delta G^\circ_b$  decreases as the ionic strength increases. The data from these curves were fitted to eq 9 using weighted nonlinear regression, and the results of these analyses are shown in Table 2. This analysis

Table 2: Parameters for the Effect of Ionic Strength on the Binding Energy of the Thrombin–Haemadin Complexes

	$C_1$	$-\Delta G_{\text{ion0}}^{\circ}$ (kJ/mol)	$-\Delta G_{\text{nio}}^{\circ}$ (kJ/mol)
native	$2.26 \pm 0.24$	$16.9 \pm 0.86$	$66.2 \pm 0.32$
K236E	$2.50 \pm 0.35$	$14.3 \pm 1.20$	$66.2 \pm 0.29$
R233E	$2.72 \pm 0.52$	$11.2 \pm 1.51$	$66.1 \pm 0.27$
K240E	$3.52 \pm 0.70$	$8.91 \pm 1.82$	$66.0 \pm 0.15$
R93E	$4.67 \pm 1.60$	$4.84 \pm 2.51$	$65.7 \pm 0.07$

Table 3: Parameters for the Effect of Ionic Strength on the Rate Constant for Association between Thrombins and Haemadin

	$C_1$	$-\Delta G_{\text{ion0}}^{\circ}$ (kJ/mol)	$k_{\text{on8}}$ ( $\times 10^7 \text{ M}^{-1} \text{ s}^{-1}$ )	$k_{\text{off}}$ ( $\times 10^{-5} \text{ s}^{-1}$ )
native	$2.37 \pm 0.37$	$17.7 \pm 2.61$	$1.00 \pm 0.12$	$2.51 \pm 0.22$
K236E	$1.99 \pm 0.20$	$11.8 \pm 0.73$	$1.00 \pm 0.08$	$2.89 \pm 0.38$
R233E	$2.16 \pm 0.40$	$8.64 \pm 1.21$	$1.14 \pm 0.10$	$3.29 \pm 0.47$
K240E	$2.44 \pm 0.41$	$6.75 \pm 0.98$	$1.14 \pm 0.06$	$3.54 \pm 0.33$
R93E	$1.90 \pm 1.52$	$1.85 \pm 0.78$	$1.09 \pm 0.11$	$3.64 \pm 0.48$

allowed the binding energy ( $\Delta G_{\text{b}}^{\circ}$ ) to be divided into a nonionic component ( $\Delta G_{\text{nio}}^{\circ}$ ) and an ionic component ( $\Delta G_{\text{ion0}}^{\circ}$ ). As Table 2 shows, of the five thrombins that were analyzed, the  $\Delta G_{\text{nio}}^{\circ}$  values are very similar, and have a weighted mean value of  $-65.8 \pm 0.10$  kJ/mol, which suggests that the mutations that have been made have only affected the ionic interactions between the proteins. However, the  $\Delta G_{\text{ion0}}^{\circ}$  values of native thrombin and the mutants were different in each case, which suggests that the binding energies for these particular amino acids are different with respect to their binding to the tail of haemadin. Examination of the  $C_1$  values shows a general increase as the binding energies of the mutants decrease.

In addition, these mutants were used to evaluate the effect of ionic strength on the associative rate constant  $k_{\text{on}}$ , these data being shown in Figure 1B, which shows that the association rate constant  $k_{\text{on}}$  decreased as the ionic strength was increased. The data from these curves were fitted by weighted nonlinear regression according to eq 10, and the results of these analyses are shown in Table 3. The results of these analyses gave the values of  $k_{\text{on8}}$  for thrombin and the thrombin mutants, this value representing the  $k_{\text{on}}$  at an infinite ionic strength where only nonionic forces play a role in the association between the molecules. These figures as shown in Table 3 are remarkably close, having a weighted mean value of  $(1.08 \pm 0.08) \times 10^7 \text{ M}^{-1} \text{ s}^{-1}$ . The analysis of these data allowed another set of figures for  $\Delta G_{\text{ion0}}^{\circ}$  to be obtained. The figures from both analyses were generally in agreement in the case of native thrombin, but in the case of the mutant thrombins, the figures were an average of 2.56 kJ/mol lower than the ones derived from Figure 1B. The  $C_1$  values for the complexes from Table 3 were generally quite similar, having a weighted mean value of  $2.14 \pm 0.30$ .

In general, when the data from Figure 1A were fitted to the Debye–Hückel equation (eq 7) and the data from Figure 1B were fitted to the Debye–Hückel version of eq 10  $\{\ln k_{\text{on}} = \ln k_{\text{on8}}(-\Delta G_{\text{ion0}}^{\circ}/RT)(\exp(-C_1\sqrt{I}))\}$ , the sum of the squares and the standard errors were slightly higher than when eqs 8 and 10 were used. In all cases, the  $C$  values were  $\sim 60\%$  higher and the  $\Delta G_{\text{ion0}}^{\circ}$  values were on average  $\sim 15\%$  lower, while the  $\Delta G_{\text{nio}}^{\circ}$  and  $k_{\text{on8}}$  values were approximately the same.

The removal of the C-terminal tail of haemadin required a specific cleavage strategy to produce a pure product for

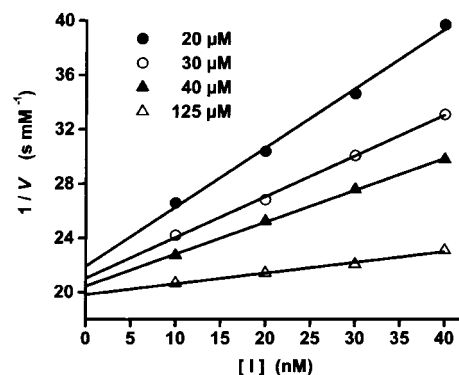


FIGURE 2: Dixon plot of human  $\alpha$ -thrombin inhibition by haemadin(1–40) at four chromagenic substrate concentrations. Points are experimental, and the lines represent the best fit by linear regression. In all cases, the linear regression coefficients were  $>99\%$ .

Table 4: Values of Kinetic Constants at Extremes of Ionic Strength for Thrombin and Haemadin Derivatives

complex/parameter	$I^a = 0.0695$	$I^a = 0.5195$
haemadin(1–40)–thrombin/ $K_i$ ( $\times 10^{-9} \text{ M}$ )	$4.93 \pm 0.14$	$5.67 \pm 0.16$
haemadin(1–40)–thrombin/ $k_{\text{on}}$ ( $\times 10^5 \text{ M}^{-1} \text{ s}^{-1}$ )	$2.76 \pm 0.22$	$2.43 \pm 0.23$
haemadin–DIP–thrombin/ $K_i$ ( $\times 10^{-8} \text{ M}$ )	$1.76 \pm 0.11$	$12.3 \pm 0.74$

<sup>a</sup>  $I$  is ionic strength.

kinetic analysis. The amino acid sequence of haemadin contains one arginine and four lysine residues, of which the N-terminal head region of haemadin contains both a lysine and arginine. Therefore, the use of trypsin-like enzymes to cleave off the C-terminal tail region of haemadin would have also cleaved off the N-terminal head of the inhibitor. Likewise, the presence of hydrophobic amino acids (proline, glutamic acid, or aspartic acid) either in the N-terminal region or in haemadin's loops made the use of other enzymes such as chymotrypsin, proline endopeptidase, endoproteinase Glu-C, and endoproteinase Asp-N also unattractive. However, the presence of an aspartic acid–proline bond allowed the selective hydrolysis of haemadin with 70% formic acid. After purification, the product was characterized by N-terminal sequencing, as well as by mass spectroscopy, with the purity being confirmed by quantitative N-terminal analysis with IleI being greater than 99%.

The resulting product haemadin(1–40) no longer exhibited tight binding inhibition, but was still a competitive inhibitor, and its  $K_i$  was determined from a plot of  $1/V$  against inhibitor concentration (Dixon plot) as shown in Figure 2. As seen in Table 4, haemadin(1–40) possesses an inhibition constant 20000 times higher than that of intact haemadin [ $(4.93 \pm 0.14) \times 10^{-9} \text{ M}$  compared to  $(2.44 \pm 0.14) \times 10^{-13} \text{ M}$ ], indicating that loss of the acidic tail severely impairs haemadin(1–40) binding to human  $\alpha$ -thrombin. A similar situation was seen for the  $k_{\text{on}}$ , which was less for haemadin(1–40) [ $(2.76 \pm 0.22) \times 10^5 \text{ M}^{-1} \text{ s}^{-1}$ ] than for intact haemadin [ $(9.32 \pm 1.65) \times 10^7 \text{ M}^{-1} \text{ s}^{-1}$ ].

With haemadin binding at sites distinct from the active site ( $I$ ), thrombin with a modified active site would be expected to compete with  $\alpha$ -thrombin for the formation of a complex with haemadin. Indeed, the inclusion of DIP-thrombin in steady state measurements caused an increase

in the  $K_i$ , which was linear when plotted against the concentration of DIP-thrombin added (data not shown). The alteration of thrombin's active site using DIPF caused a 72000-fold increase in the  $K_i$  of the inhibitor [from  $(1.76 \pm 0.11) \times 10^{-8}$  to  $(2.44 \pm 0.14) \times 10^{-13}$  M], indicating that haemadin binds to DIP-thrombin less strongly than to  $\alpha$ -thrombin.

The kinetic constants of the human  $\alpha$ -thrombin–haemadin(1–40) complex and the human DIP- $\alpha$ -thrombin–haemadin complex at two different ionic strengths are shown in Table 4 for comparison. In particular, it is noteworthy that haemadin(1–40) shows little change in either its  $K_i$  (from  $4.93 \pm 0.14$  to  $5.67 \pm 0.16$  M) or its  $k_{on}$  (from  $2.76 \pm 0.22$  to  $2.43 \pm 0.23$  M<sup>-1</sup> s<sup>-1</sup>) at low (0.0695) or high (0.5195) ionic strengths.

The synthetic amino terminal peptides (H-IRFGMGKV-NH<sub>2</sub> and H-IRFGMGKVP-NH<sub>2</sub>) based on the first eight and nine amino acids of haemadin, respectively, had  $K_i$  values in the micromolar range [ $(3.27 \pm 0.30) \times 10^{-6}$  and  $(3.01 \pm 0.14) \times 10^{-6}$  M, respectively].

## DISCUSSION

We have recently determined the three-dimensional crystal structure of the human  $\alpha$ -thrombin–haemadin complex, which revealed that haemadin binds both to exosite II of thrombin and to the active site, making it a unique inhibitor of thrombin (11). However, due to crystal contacts, the exact nature of the binding of the C-terminal tail of haemadin to thrombin was not revealed.

The primary aim of this work was to determine the component of the binding energy of the human  $\alpha$ -thrombin–haemadin complex that is due to ionic interactions, and how many of these ionic interactions are from the acid rich tail of haemadin. Knowledge of the binding energy of the C-terminal tail and the average distance between these interactions should enable us to estimate how many ionic bonds it forms with exosite II. Also considered was the relative importance of the C-terminal peptide compared to the N-terminal peptide of haemadin when it binds to thrombin.

It is useful when referring to haemadin to compare it with another leech inhibitor, hirudin, a 65-amino acid protein from the medicinal leech *Hirudo medicinalis* (31), due to their similarities, particularly in their folds, and in their noncanonical modes of binding of their N-termini to the active site of thrombin. However, these two leech-derived peptides differ drastically when it comes to the binding location of their acidic C-terminal peptides, with hirudin binding to exosite I and haemadin to the diametrically opposite exosite II (11).

At an infinite ionic strength, the  $K_i$  values for complexes of haemadin and recombinant hirudin (calculated from ref 13) with human  $\alpha$ -thrombin are  $2.97 \times 10^{-12}$  and  $1.87 \times 10^{-11}$  M, or 6.3 times higher for hirudin, indicating haemadin is the better binder at an infinite ionic strength. At a blood ionic strength (~154 mM), the  $K_i$  values are  $2.91 \times 10^{-13}$  and  $5.65 \times 10^{-13}$  M, with recombinant hirudin [the clinically approved form of hirudin (32)] being about half that of haemadin. The comparison of  $k_{on}$  values at a physiological ionic strength shows a slightly lower  $k_{on}$  value for haemadin ( $4.28 \times 10^7$  M<sup>-1</sup> s<sup>-1</sup> compared to  $6.39 \times 10^7$  M<sup>-1</sup> s<sup>-1</sup> for

recombinant hirudin). These  $k_{on}$  values for thrombin inhibitors have been shown to be more important for therapeutic usage than the  $K_i$  value for in vivo thrombin inhibition, due to the concentration of thrombin in the thrombus (33, 34).

The weighted mean  $k_{on8}$  for the haemadin complexes from Table 2, compared to those of hirudin complexes (13), is  $(1.08 \pm 0.08) \times 10^7$  M<sup>-1</sup> s<sup>-1</sup> versus  $(1.32 \pm 0.25) \times 10^6$  M<sup>-1</sup> s<sup>-1</sup>, or 8 times higher. This indicates that the high  $k_{on}$  of the human  $\alpha$ -thrombin–haemadin complex is less dependent on ionic forces than it is for the human  $\alpha$ -thrombin–hirudin complex.

The  $k_{off}$  figures for all the human  $\alpha$ -thrombin–haemadin complexes were similar, having a weighted mean of  $(2.73 \pm 0.40) \times 10^{-5}$  s<sup>-1</sup> which is comparable to the figure for recombinant hirudin [ $0.98 \times 10^{-5}$  s<sup>-1</sup> (35)]. The major kinetic difference between the complexes is in the  $k_{on}$ , the values of which for both complexes have different profiles when plotted against ionic strength.

The weighted mean of the  $-\Delta G^{\circ}_{ion0}$  from Tables 2 and 3 of  $-16.96 \pm 0.96$  kJ/mol shows that ionic interactions make up 20% of the total binding energy at zero ionic strength of the human  $\alpha$ -thrombin–haemadin complex.

Haemadin(1–40) binding being virtually unaffected by ionic strength (see Table 4) indicates that the majority of the ionic interactions come from the tail region of haemadin. Additional proof for this hypothesis is that DIP-thrombin binding to intact haemadin is dependent on ionic strength (see Table 4). The difference in binding energies for the DIP-thrombin–haemadin complex at ionic strengths of 0.0695 and 0.5195 is 4.82 kJ/mol. This figure is close to the difference in the binding energies of the human  $\alpha$ -thrombin–haemadin complex at the same ionic strengths, which is 4.56 kJ/mol. Yet further proof comes from the fact that the  $k_{on}$  values for haemadin(1–40) are virtually unchanged at ionic strengths of 0.0695 and 0.5195 (see Table 4).

Knowing that haemadin's C-terminal tail is responsible for most of the  $-16.96 \pm 0.96$  kJ of ionic interactions at an ionic strength of zero allows us to estimate how many ionic interactions take place. Using a figure of -4.0 kJ per participating ionic contribution, as for the tail of hirudin and exosite I of thrombin<sup>4</sup> (13), this converts to approximately four residues playing a role in interactions with exosite II. This figure is close to our observations where the four mutants present in Tables 2 and 3 (Arg93, Lys236, Arg233, and Lys240), as well as Arg101 (as in the crystal structure), are all implicated in ionic binding of haemadin to thrombin.

A more accurate assessment comes from the fact that by Debye–Hückel theory the constant  $C_1$  should be equal to one-third of the separation distance between the charges (13). Using the weighted mean of the  $C_1$  values for the native human  $\alpha$ -thrombin–haemadin complex ( $2.29 \pm 0.27$ ) to obtain this distance, and substituting it into eq 11, gives an average energy of an ionic interaction of -2.53 kJ/mol. If the  $\Delta G^{\circ}_{ion0}$  of the human  $\alpha$ -thrombin–haemadin complex ( $-16.96 \pm 0.96$  kJ) is divided by this number, it yields an even higher number, 6.7, as the number of ionic interactions in the complex. Interestingly, this number is close to the value derived from reported data from the human  $\alpha$ -thrombin–

<sup>4</sup> The crystal structure of the human  $\alpha$ -thrombin–hirudin complex (PDB entry 1HTC) contains almost no direct salt bridges, but contains several indirect ones.



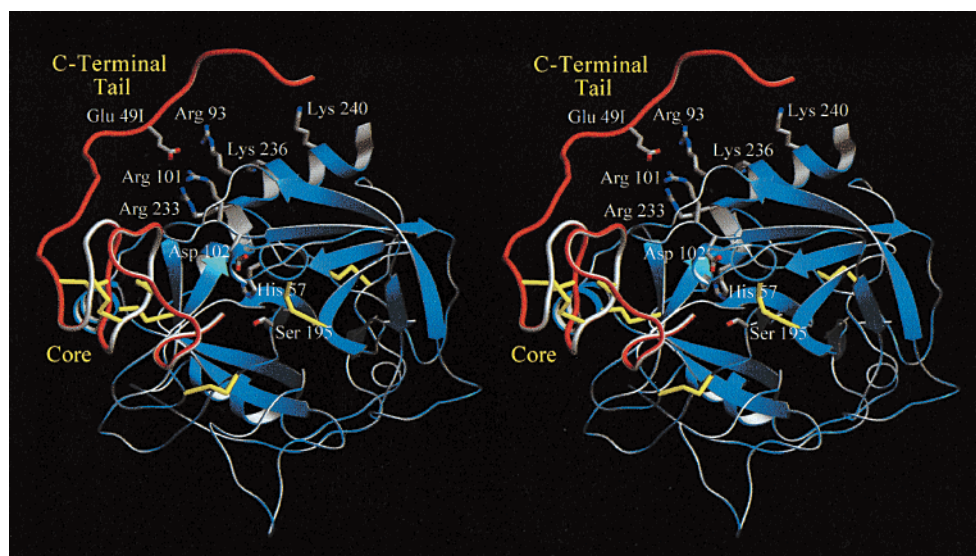


FIGURE 3: X-ray structure of the human  $\alpha$ -haemadin complex. Haemadin is depicted as a red and white rope with its C-terminal tail and core region being explicitly labeled, as well as residue Glu491 which forms a salt bridge with Arg101 of thrombin in the complex. Thrombin is shown in blue and white, in the “standard orientation” (40), i.e., with the active site cleft facing the viewer and substrates running from left to right. Shown explicitly are the basic side chains of thrombin which have been mutated to glutamic acid, which consequently increases the  $K_i$  of the complex. Also shown are the catalytic triad (Asp102, His57, and Ser195) into which haemadin inserts its N-terminal peptide. This figure was prepared with SETOR (41).

recombinant hirudin complex (13), where the result is 6.25. The 2-fold higher  $C_1$  value of haemadin compared to that of hirudin (13) shows that the C-terminal tail of haemadin is not as tightly bound by ionic forces.

However, calculation of the distance between charges for the human  $\alpha$ -thrombin–hirudin complex using eq 11, the distance is 4.3 Å (13), which is 66% of the figure for the human  $\alpha$ -thrombin–haemadin complex. These distances appear to be correct when the X-ray structures are inspected, with the C-terminal tail of hirudin being closer to thrombin than the C-terminal tail of haemadin (PDB entries 1E0F and 1HTC).

Concerning the N-terminal peptide of haemadin, DIP-thrombin has a 72000-fold reduced affinity for haemadin, this figure being higher than the 20000-fold reduced affinity haemadin(1–40) has for thrombin. This indicates that the amino-terminal peptide of haemadin is more important for binding than the tail region. The synthetic amino-terminal peptides based on the first eight and nine amino acids of haemadin are reasonably strong inhibitors of thrombin, having  $K_i$  values in the micromolar range.  $\Delta G^\circ_b$  values of  $-31.31$  and  $-31.52$  kJ, respectively, closely match the loss of free energy due to thrombin being blocked by diisopropyl fluorophosphate, which is 27.74 kJ. This figure is larger than for the DIP-thrombin–hirudin complex, which loses 18 kJ/mol of binding energy under the same conditions (22), indicating that haemadin binds more strongly to the active site than hirudin.

The  $K_i$  of the human  $\alpha$ -thrombin–haemadin(1–40) complex is  $\sim 2$  orders of magnitude stronger than those of the equivalently cleaved peptide complexes from HM2(1–41) [ $K_i = (400 \pm 50) \times 10^{-9}$  M (36)] and hirudin(1–43) [ $K_i = (299 \pm 12) \times 10^{-9}$  M (37)], which suggests that the C-terminal tail of haemadin is less important for binding to thrombin than that of hirudin or HM2.

Removal of the tail of haemadin causes a 24.58 kJ decrease in the binding energy, and this decrease is larger than the

binding energy ( $\Delta G^\circ_{ion}$ ) of the ionic binding contributions in the human  $\alpha$ -thrombin–haemadin complex, which at the same ionic strength (0.0695) is equal to  $-5.83 \pm 0.28$  kJ/mol. This 5-fold disparity indicates that the C-terminal tail of haemadin contributes more than just ionic interactions to the energy of binding. This additional loss of energy may be attributable to the large reduction in the  $k_{on}$  of the complex, which decreases 338-fold. The corresponding change in  $k_{off}$  values is only a 60-fold increase, indicating that the C-terminal tail of haemadin has greater implications for the  $k_{on}$  than for the  $k_{off}$ .

From Tables 2 and 3, it is evident that there is not an equal energy loss upon haemadin binding to each mutant, which suggests that the ionic interactions are specific in nature. These results are in line with those from hirudin mutants, where ionic residues mutated to neutral residues caused different changes in the  $\Delta G^\circ_b$  values in their complexes with human  $\alpha$ -thrombin (35).

In conclusion, the contribution of ionic interactions in the human  $\alpha$ -thrombin–haemadin complex is much smaller than for the human  $\alpha$ -thrombin–hirudin complex, with it relying much less on ionic interactions in forming a tight complex and in its rate of association with thrombin. At least five residues in the C-terminal tail of haemadin interact using ionic forces with thrombin, which is similar to the number that hirudin utilizes, the major difference being that the binding distances are 50–100% greater for haemadin. As shown in Figure 3, the location of haemadin’s C-terminal tail is approximately correct in terms of its location with respect to residues with which it is known to interact, and in terms of its distance from them.

Unlike in hirudin, ionic interactions are not as vital for haemadin’s high rate of association with thrombin, which both inhibitors achieve through their C-terminal tails. Thus, the tail of haemadin can be seen as an orienting structure, but using fewer long-range ionic forces to orient it than hirudin. This suggests that other factors, such as some form

of cooperativity in binding, play a role in the rate of association, as has been seen for ionic residues in the human  $\alpha$ -thrombin–hirudin complex (38). In this way, the haemadin's C-terminal tail may differ from hirudin's tail which is in a stable conformer when it binds to thrombin (39), whereas haemadin's may actively seek an orientation; this seeking behavior may also apply to its N-terminal peptide.

## REFERENCES

1. Davie, E. W., Fujikawa, K., and Kisiel, W. (1991) *Biochemistry* 30, 10363–10370.
2. Vu, T. K., Hung, D. T., Wheaton, V. I., and Coughlin, S. R. (1991) *Cell* 64, 1057–1068.
3. Coughlin, S. R. (1999) *Proc. Natl. Acad. Sci. U.S.A.* 96, 11023–11027.
4. Ramakrishnan, V., DeGuzman, F., Bao, M., Hall, S. W., Leung, L. L., and Phillips, D. R. (2001) *Proc. Natl. Acad. Sci. U.S.A.* 98, 1823–1828.
5. Kane, W. H., and Davie, E. W. (1988) *Blood* 71, 539–555.
6. Gailani, D., and Broze, G. J., Jr. (1991) *Science* 253, 909–912.
7. Esmon, C. T. (1995) *FASEB J.* 9, 946–955.
8. Nesheim, M., Wang, W., Boffa, M., Nagashima, M., Morser, J., and Bajzar, L. (1997) *Thromb. Haemostasis* 78, 386–391.
9. Bode, W., Mayr, I., Baumann, U., Huber, R., Stone, S. R., and Hofsteenge, J. (1989) *EMBO J.* 8, 3467–3475.
10. Strube, K. H., Kröger, B., Bialojan, S., Otte, M., and Dodt, J. (1993) *J. Biol. Chem.* 268, 8590–8595.
11. Richardson, J. L., Kröger, B., Hoeffken, W., Sadler, J. E., Pereira, P., Huber, R., Bode, W., and Fuentes-Prior, P. (2000) *EMBO J.* 19, 5650–5660.
12. Schechter, I., and Berger, A. (1967) *Biochem. Biophys. Res. Commun.* 27, 157–162.
13. Stone, S. R., Dennis, S., and Hofsteenge, J. (1989) *Biochemistry* 28, 6857–6863.
14. Owen, W. G., and Jackson, C. M. (1973) *Thromb. Res.* 3, 705–714.
15. Sheehan, J. P., and Sadler, E. J. (1994) *Proc. Natl. Acad. Sci. U.S.A.* 91, 5518–5522.
16. Sheehan, J. P., Wu, Q., Tollefsen, D. M., and Sadler, J. E. (1993) *J. Biol. Chem.* 268, 3639–3645.
17. Jameson, G. W., Roberts, D. V., Adams, R. W., Kyle, W. S. A., and Elmore, D. T. (1973) *Biochem. J.* 131, 101–117.
18. Ellis, K. J., and Morrison, J. F. (1982) *Methods Enzymol.* 87, 405–426.
19. Segel, I. H. (1975) *Enzyme Kinetics*, John Wiley and Sons, New York.
20. Gill, S. G., and von Hippel, P. H. (1989) *Anal. Biochem.* 182, 319–326.
21. Myles, T., Church, F. C., Whinna, H. C., Monard, D., and Stone, S. R. (1998) *J. Biol. Chem.* 273, 31203–31208.
22. Stone, S. R., Braun, P. J., and Hofsteenge, J. (1987) *Biochemistry* 26, 4617–4624.
23. Fenton, J. W., II, Fasco, M. J., Stackrow, A. B., Aronson, D. L., Young, A. M., and Finlayson, J. S. (1977) *J. Biol. Chem.* 252, 3587–3598.
24. Williams, J. W., and Morrison, J. F. (1979) *Methods Enzymol.* 63, 437–467.
25. Morrison, J. F. (1982) *Trends Biochem. Sci.* 7, 102–105.
26. Adamson, A. W. (1979) *Textbook of Physical Chemistry*, pp 461–478, Academic Press, New York.
27. Meyer, T. E., Watkins, J. A., Przysiecki, C. T., Tollin, G., and Cusanovich, M. A. (1984) *Biochemistry* 23, 4761–4767.
28. Tollin, G., Cheddar, G., Watkins, J. A., Meyer, T. E., and Cusanovich, M. A. (1984) *Biochemistry* 23, 6345–6349.
29. Przysiecki, C. T., Cheddar, G., Meyer, T. E., Tollin, G., and Cusanovich, M. A. (1985) *Biochemistry* 24, 5647–5652.
30. Laidler, K. J. (1987) *Chemical Kinetics*, pp 191–194, Harper and Row, New York.
31. Rydel, T. J., Ravichandran, K. G., Tulinsky, A., Bode, W., Huber, R., Roitsch, C., and Fenton, J. W., II (1990) *Science* 249, 277–280.
32. Salzet, M. (2001) *FEBS Lett.* 492, 187–192.
33. Elg, M., Gustafsson, D., and Deinum, J. (1997) *Thromb. Haemostasis* 78, 1286–1292.
34. Stone, S. R., and Tapparelli, C. (1995) *J. Enzyme Inhib.* 9, 3–15.
35. Braun, P. J., Dennis, S., Hofsteenge, J., and Stone, S. R. (1988) *Biochemistry* 27, 6517–6522.
36. Vindigni, A., De Filippis, V., Zanotti, G., Visco, C., Orsini, G., and Fontana, A. (1994) *Eur. J. Biochem.* 226, 323–333.
37. Chang, J. Y., Schlaeppli, J. M., and Stone, S. R. (1990) *FEBS Lett.* 260, 209–212.
38. Myles, T., Le Bonniec, B. F., Betz, A., and Stone, S. R. (2001) *Biochemistry* 40, 4972–4979.
39. Ni, F., Ripoll, D. R., and Purisima, E. O. (1992) *Biochemistry* 31, 2545–2554.
40. Bode, W., and Huber, R. (1992) *Eur. J. Biochem.* 204, 433–451.
41. Evans, S. V. (1990) *J. Mol. Graphics* 11, 134–138.

BI011605Q